

The Interaction of Recombinant Subdomains of the Procollagen C-Proteinase with Procollagen I Provides a Quantitative Explanation for Functional Differences between the Two Splice Variants, Mammalian Tolloid and Bone Morphogenetic Protein 1[†]

Vera Hintze,^{‡,§,||} Markus Höwel,^{‡,§,⊥} Carsten Wermter,[‡] Eva Grosse Berkhoff,[@] Christoph Becker-Pauly,[‡] Bernd Beermann,[#] Irene Yiallourous,[‡] and Walter Stöcker^{*,‡}

Department I, Cell and Matrix Biology, Institute of Zoology, Johannes Gutenberg-University, D-55099 Mainz, Germany, and Institutes of Zoophysiology and Physical Chemistry, Westfälische Wilhelms-University, D-48149 Münster, Germany

Received February 3, 2006; Revised Manuscript Received March 22, 2006

ABSTRACT: The procollagen C-proteinase (PCP) is a zinc peptidase of the astacin family and the metzincin superfamily. The enzyme removes the C-terminal propeptides of fibrillar procollagens and activates other matrix proteins. Besides its catalytic protease domain, the procollagen C-proteinase contains several C-terminal CUB modules (named after complement factors C1r and C1s, the sea urchin UEGF protein, and BMP-1) and EGF-like domains. The two major splice forms of the C-proteinase differ in their overall domain composition. The longer variant, termed mammalian tolloid (mTld, i.e., PCP-2), has the protease-CUB1-CUB2-EGF1-CUB3-EGF2-CUB4-CUB5 composition, whereas the shorter form termed bone morphogenetic protein 1 (BMP-1, i.e., PCP-1) ends after the CUB3 domain. Two related genes encode proteases similar to mTld in humans and have been termed mammalian tolloid like-1 and -2 (mTll-1 and mTll-2, respectively). For mTll-1, it has been shown that it has C-proteinase activity. We demonstrate that recombinant EGF1-CUB3, CUB3, CUB3-EGF2, EGF2-CUB4, and CUB4-CUB5 modules of the procollagen C-proteinase can be expressed in bacteria and adopt a functional antiparallel β -sheet conformation. As shown by surface plasmon resonance analysis, the modules bind to procollagen I in a 1:1 stoichiometry with dissociation constants (K_D) ranging from 622.0 to 1.0 nM. Their binding to mature collagen I is weaker by at least 1 order of magnitude. Constructs containing EGF domains bind more strongly than those consisting of CUB domains only. This suggests that a combination of CUB and EGF domains serves as the minimal functional unit. The binding affinities of the EGF-containing modules for procollagen increase in the order EGF1-CUB3 < CUB3-EGF2 < EGF2-CUB4. In the context of the full length PCP, this implies that a given module has an affinity that continues to increase the more C-terminally the module is located within the PCP. The tightest binding module, EGF2-CUB4 (K_D = 1.0 nM), is only present in mTld, which might provide a quantitative explanation for the different efficiencies of BMP-1 and mTld in procollagen C-proteinase activity.

Procollagen C-proteinase (PCP)¹ was first purified as a 100 kDa protein (PCP-2) from chicken embryo tendons (1) and later as a 70 kDa (PCP-1) protein from mouse fibroblasts

(2). Bone morphogenetic protein 1 (BMP-1) was originally identified as a zinc metalloprotease in extracts of demineralized bovine bone together with TGF β -like growth factors, termed BMP-2A and BMP-3 (3). Amino acid sequencing and cDNA cloning demonstrated that mouse PCP-1 was identical to BMP-1 and chicken PCP-2 was identical to a protein named mTld (mammalian tolloid) after the homologous *Drosophila* proteinase tolloid (4–6). These enzymes are two of six known splice variants of the *bmp1* gene (7).

[†] This work has been supported by a research grant from the Deutsche Forschungsgemeinschaft (SFB 492 A5, to W.S.). V.H. acknowledges research stipends from the Schering Forschungsgesellschaft (Berlin, Germany) and from the Heinrich-Hertz Foundation (Düsseldorf, Germany). M.H. is grateful for support by the Hermann Schlosser Foundation (Dortmund, Germany). We thank Dr. Elmar R. Burchhard and Dr. Stephan Kauschke for support and discussions.

^{*} To whom correspondence should be addressed: Institute of Zoology, Johannes Gutenberg-University, D-55099 Mainz, Germany. Telephone: +49-6131-3924273. Fax: +49-6131-3923835. E-mail: stoecker@uni-mainz.de.

[‡] Johannes Gutenberg-University.

[§] These authors contributed equally to this work.

^{||} Present address: Department of Dermatology and Cutaneous Biology, Thomas Jefferson University, Philadelphia, PA 19107.

[⊥] Present address: Department of Dermatology, University Hospital, D-48149 Münster, Germany.

[@] Institute of Zoophysiology, Westfälische Wilhelms-University.

[#] Institute of Physical Chemistry, Westfälische Wilhelms-University.

¹ Abbreviations: aSFP, acidic seminal protein; BMP-1, bone morphogenetic protein 1; CUB, protein module named according to its presence in complement factors C1r and C1s, the sea urchin UEGF protein, and BMP-1; DTT, dithiothreitol; E64, *trans*-epoxysuccinyl-L-leucylamido(4-guanidino)butane; EGF, epidermal growth factor; IPTG, isopropyl β -D-thiogalactopyranoside; PCP, procollagen C-proteinase; PCPE, procollagen C-proteinase enhancer; MBP, collagen-like mannose-binding protein; MASP-2, mannose-binding associated serine proteinase-2; mTld, mammalian tolloid; mTll, mammalian tolloid-like; PMSF, phenylmethanesulfonyl fluoride; PSPI/PSPII, porcine sperm adhesion protein; TGF β , transforming growth factor β .

BMP-1, mTld, and mTll-1 are critical for the assembly of the extracellular matrix because they cleave the propeptides of fibrillar collagens I–III, V, and XI (1, 5, 6, 8–11), as well as the small, leucine-rich proteoglycan probiglycan (12). They also cleave procollagen VII (13) and the α_3 - and γ_2 -chains of prolaminin 5 (14, 15), thereby facilitating the assembly of the dermal–epidermal junction and of anchoring fibrils. Furthermore, BMP-1/tolloid-like proteases play important roles in cross-linking collagens and elastin by activating the prolyl-oxidase (16, 17). In embryonic development, these enzymes are crucial in dorso-ventral patterning because they release ventralizing TGF β -like factors from their antagonist chordin in vertebrates (18–21) and dorsalizing growth factors in *Drosophila* (22). Hence, the C-proteinase seems to orchestrate the assembly of the extracellular matrix and patterning events (23).

Two related genes encoding proteases similar to mTld have been identified in *bmp1* null mice and have been termed mammalian tolloid like-1 and -2 (mTll-1 and mTll-2, respectively). The *bmp1*^{−/−} mice have abnormal collagen fibrillogenesis in skin and are perinatal lethal due to incomplete ventral body wall closure (24). However, they do develop a skeleton due to mTll-1, which also exhibits C-proteinase activity and can partially compensate for the loss of the *bmp1* gene (24).

The procollagen C-proteinase is a member of the astacin family and the metzincin superfamily of zinc peptidases (25–27). Unlike the archetypal crayfish enzyme astacin, which consists solely of a compact protease domain, the C-proteinase contains EGF-like domains and CUB modules (28, 29). The two major splice variants differ in the number of these domains. In PCP-1/BMP-1, the sequential order of the domains is as follows: protease, CUB1, CUB2, EGF1, and CUB3. The variant PCP-2/mTld is elongated C-terminally with EGF2, CUB4, and CUB5.

CUB-EGF entities have been reported to mediate protein–protein interactions also involving collagen-like structures. For example, the CUB-EGF moieties of complement proteins C1r and C1s form a head-to-tail heterodimer, which interacts with the collagen-like C1q protein (30, 31). The CUB1-EGF-CUB2 modules of the mannose-binding protein-associated serine protease 2 (MASP-2) mediate homodimerization and interaction with the collagen-like mannose-binding protein (MBP) (32). The CUB modules of C1s (31) and MASP-2 (32) have a typical antiparallel β -sheet structure that is highly similar to the sperm adhesin PSPI–PSPII heterodimer (porcine sperm adhesion protein) and to aSFP (acidic seminal protein) (33).

There is evidence that the different CUB and EGF domains play distinct parts in the overall function of the C-proteinase, since the differences in their amino acid sequences and modeling studies based on the structure of PSPI/PSPII identify them as individual entities (34). However, the roles of the C-terminal domains are still obscure, since there are contradictory reports in the literature. For example, it has been published that CUB1 is essential for secretion, that a C-proteinase lacking the CUB2 domain is a poor protease, and that the activity of the enzyme is completely abolished if the CUB2-EGF1-CUB3 module is missing (35). On the other hand, a more recent paper has shown that the protease domain of BMP1 alone can be secreted and exhibit C-proteinase activity (36).

Albeit derived from the same gene, BMP-1 and mTld do not exhibit the same substrate specificity. For example, BMP-1 has been shown to be a more efficient C-proteinase and chordinase than mTld (20). This paradox has recently been addressed by Kadler and co-workers (37), who found that deletion of the EGF-like domains in mTld converted the enzyme into a more effective C-proteinase, similar to BMP-1.

In this study, we sought to acquire quantitative data on the interaction of the procollagen C-proteinase with its main substrate, procollagen I. For this purpose, we cloned the cDNAs encoding several C-terminal subfragments, which overlap each other successively. The modules were expressed in *Escherichia coli* and folded in vitro. As deduced from circular dichroism spectra, the modules consist mainly of antiparallel β -sheets. Kinetic analysis by a surface plasmon resonance methodology demonstrated that the modules bind to procollagen I and collagen I with strikingly different affinities. The data indicate that the EGF-like domains strongly enhance binding and that the tightest interaction is seen with the EGF2-CUB4 module, a construct present only in mTld but not in BMP-1. These data might provide a quantitative explanation for the functional differences between the two splice variants.

MATERIALS AND METHODS

Chemicals. All chemicals were analytical grade and, if not stated otherwise, obtained from Amersham Bioscience (Freiburg, Germany), AppliChem (Darmstadt, Germany), Serva (Heidelberg, Germany), Bio-Rad (Munich, Germany), Sigma/Aldrich (Taufkirchen, Germany), New England Biolabs (Frankfurt/Main, Germany), and Merck (Darmstadt, Germany).

Cells and Plasmids. PCP-1/BMP-1 and PCP-2/mTld cDNA inserted into the pQE 70 vector (a kind gift of W. Herzog and R. Lauster, Deutsches Rheumaforschungszentrum, Berlin, Germany) were used as templates for PCR. The following primers were used for the amplification of the constructs (sequences in the 5′–3′ direction): EGF1-CUB3, GAGACATATGGTGGACGAGTGCTCTCGGCC (forward) and GAGAGGATCCTAGTGATGGTGATGGTGATGTTCTGAGAAGAAGTG (reverse); CUB3, GAGACATATGTGTGGCGGATTCCTACCAAGCTC (forward) and GAGAGGATCCTAGTGATGGTGATGGTGATGTTCTGAGAAGAAGTG (reverse); CUB3-EGF2, GAGACATATGTGTGGCGGATTCCTACCAAGCTC (forward) and GAGAGGATCCTAGTGATGGTGATGGTGATGGCCGGCTTCTTTGCAGTC (reverse); EGF2-CUB4, GAGACATATGAAGGACGAGTGCTCCAAG (forward) and GAGAGGATCCTAGTGATGGTGATGGTGATGCTCTGTGGCGTGGGAGGC (reverse); CUB4-CUB5, GAGACATATGTGTGACCACAAGGTGACA (forward) and GAGAGGATCCTAGTGATGGTGATGGTGATGCTTCTGTGGAGTGT (reverse). The primers introduce a 3′ hexa-His tag and NdeI and BamHI restriction sites at the 5′ and 3′ ends of the cDNA, respectively. The constructs were subcloned into the pGEM-T vector (Promega, Mannheim, Germany). For expression of the PCP constructs, the sequences were isolated as NdeI–BamHI fragments and ligated into the pET3a vector (Invitrogen, Karlsruhe, Germany). *E. coli* BL21(DE3) cells (Stratagene, Amsterdam, The Netherlands) were transformed

with pET3a/PCP domain plasmids, which had been established in a nonexpression host. These cells carry the T7 RNA polymerase gene (λ DE3 lysogen), which is under the control of a lacUV5 promoter. The design allows the expression of PCP domains upon induction with IPTG (isopropyl β -D-thiogalactopyranoside).

Expression of Recombinant Proteins. *E. coli* BL21(DE3) cells transformed with the PCP constructs were grown for 16–18 h in 30 mL of LB medium containing ampicillin (100 μ g/mL) in a shaking incubator at 37 °C; 100 mL of culture medium was added, and bacteria were incubated for an additional 1 h. A 20 mL sample of this culture was grown in 225–250 mL until the extinction at 600 nm (E_{600}) had reached a value of 0.7–0.9. IPTG was added to a final concentration of up to 10 mM to induce the synthesis of T7 polymerase and thus to initiate the synthesis of the PCP mRNAs. The incubation was continued for 4 h. Cells were harvested by centrifugation at 4500g for 15 min at 4 °C.

Protein Purification and Folding. Purification and folding of recombinant bacterial proteins were essentially performed as described previously (38). Briefly, 3 g of harvested pellet was solubilized by adding lysis buffer consisting of 50 mL of 0.05 M Tris-HCl (pH 8.0), 6 M guanidinium chloride, 0.15 M NaCl, 0.02 M β -mercaptoethanol, 500 μ M PMSF (phenylmethanesulfonyl fluoride), 1 μ M pepstatin A, and 2 μ M E64 [*trans*-epoxysuccinyl-L-leucylamido(4-guanidino)-butane]. The solution was then centrifuged for 20 min at 8500g. The resulting supernatant was incubated for 16–18 h with Ni-NTA superflow (Qiagen, Hilden, Germany) in a batch procedure at 4 °C. The material was transferred into a column, and affinity chromatography was performed in the flow-through mode using a decreasing pH gradient. Washing buffers contained 0.05 mM Tris-HCl (pH 8.0, 6.3, and 5.9) with 8 M urea and 0.15 M NaCl. The elution of the domains was accomplished by shifting the pH to 4.5. Elution fractions containing 2–6 mg of the domains were dialyzed against 0.1 M NaHCO₃ and 0.5 M NaCl (pH 8.3) for EGF1-CUB3 and 5 mM ammonium acetate (pH 8.2) for CUB3-EGF2. Both procedures were performed at room temperature for 24 h, the buffer being changed three times. Folding of the other three domains was also achieved via dialysis, but with varying buffer compositions. In the case of CUB3, the first folding buffer contained 50 mM CAPS (pH 10.0), 3 M NaCl, 2 M L-arginine, 2 M sucrose, 2 mM MgCl₂, 2 mM CaCl₂, 3 mM reduced glutathione, and 0.3 mM oxidized glutathione. After 24 h, the CUB3 domain was dialyzed against 50 mM CAPS (pH 10.0), 150 mM NaCl, 2 mM MgCl₂, and 2 mM CaCl₂. The first step was performed at room temperature for 24 h and the latter at 4 °C. EGF2-CUB4 was folded at room temperature in 0.1 M NaHCO₃ (pH 8.0) supplemented with 0.08 M L-arginine, 2 M L-proline, 0.5 M sucrose, and 0.5 M NaCl for 24 h. The buffer was then changed to 0.1 M NaHCO₃ (pH 8.0) containing 0.08 M L-arginine and 0.5 M NaCl. After 4 h, 0.1 M NaHCO₃ (pH 8.0) with 0.5 M NaCl was used. CUB4-CUB5 was first dialyzed with 0.05 M NaHCO₃ (pH 8.3), 0.8 M L-arginine, 0.5 M glycerol, 0.5 M glycine, 1 M saccharose, and 0.5 M NaCl for 24 h. The buffer was then changed to 0.05 M NaHCO₃ (pH 8.3), 0.5 M glycerol, 0.5 M glycine, 1 M saccharose, and 0.5 M NaCl. After 4 h, 0.05 M NaHCO₃ (pH 8.3) and 0.5 M NaCl were used. Folding of this domain was achieved at room temperature.

SDS–Polyacrylamide Gel Electrophoresis (PAGE) and Immunoblotting. Protein samples derived from purification or folding were mixed with sample buffer, containing 0.25 M Tris-HCl (pH 6.8), 10% SDS (w/v), 35% glycerol (v/v), and bromophenol blue, supplemented with 0.75 M DTT (dithiothreitol). Samples originating from expression cultures were centrifuged at 13000g, and the cell pellet was suspended in sample buffer. The samples were boiled for 10 min and loaded on a discontinuous 15% SDS–polyacrylamide gel (39). Gels were stained with Coomassie Brilliant Blue G250.

SDS gels were blotted in a semidry blotting apparatus (Bio-Rad) onto PVDF membranes (Immobilon P, Millipore, Eschborn, Germany) using 0.3 M Tris-HCl (pH 10.4) containing 20% methanol (v/v) as the anode buffer and 0.25 M Tris-HCl (pH 8.0) with 20% methanol (v/v) as the cathode buffer. The membrane was blocked with 3% (w/v) serum albumin in TBS [Tris-buffered saline; 0.02 M Tris-HCl (pH 7.4)]. For detection of PCP domains, an anti-His tag mouse IgG antibody (Qiagen) was dissolved in blocking buffer. Peroxidase-labeled sheep anti-mouse IgG in TBS containing 10% (w/v) skim milk powder was used as a second antibody. The bands were detected using a chemoluminescence peroxidase substrate (ECL, Amersham Life Science, Freiburg, Germany).

Protein Sequencing. N-Terminal Edman sequencing was performed by SeqLab (Göttingen, Germany).

Fluorescence Spectroscopy. The folding state of the domains was monitored using fluorescence spectroscopy. Excitation of tryptophan indole rings was performed at 25 °C and 280 nm with a slit width of 2.5 nm in an LS 50 B spectrometer (Perkin Elmer, Norwalk, CT). Emission was recorded between 300 and 500 nm. Values of 10 scans were averaged.

Circular Dichroism (CD) Spectroscopy. CD spectra were measured at 20 °C with a Jobin-Yvon (Paris, France) spectropolarimeter equipped with a cuvette with a path length of 0.5 mm. The protein concentration was adjusted to 0.6–0.7 mg/mL. The spectra of the buffers were subtracted from the spectra of the respective protein solution. Data were submitted to deconvolution using CDNN (40) to determine secondary structure elements.

Surface Plasmon Resonance Analysis. Real-time analysis of the interaction of PCP domains with human procollagen I (a gift of L. Bruckner-Tuderman, Department of Dermatology, University of Freiburg, Freiburg, Germany) was performed at 25 °C using a BIAcore (Uppsala, Sweden) 3000 instrument. Procollagen I (8.6 μ g/mL) in 0.01 M Hepes (pH 3.0) was coupled to the carboxymethylated dextran surface of a CM5 sensor chip using amine coupling chemistry according to the manufacturer's instructions. Immobilization of proteins was achieved in HBS-EP buffer [0.01 M Hepes (pH 7.4), 0.15 M NaCl, 3 mM EDTA, and 0.005% polysorbate 20 (v/v)] at a flow rate of 5 μ L/min up to a level of 780 resonance units (RU). Collagen I (0.4 μ g/mL, Sigma) in 0.01 M Hepes (pH 5.0) was coupled to a CM5 sensor chip surface using the same procedure to a level of 2090 RU. Binding was achieved in 0.01 M Hepes (pH 7.4) with 0.15 M NaCl, 5 mM CaCl₂, and 0.005% polysorbate 20 (v/v) for all PCP domains: EGF1-CUB3 (150–850 nM), CUB3 (200–1300 nM), CUB3-EGF2 (375–750 nM), EGF2-CUB4 (200–1000 nM), and CUB4-CUB5 (200–800 nM). Sixty microliters of analyte was injected at a flow rate of 5 μ L/

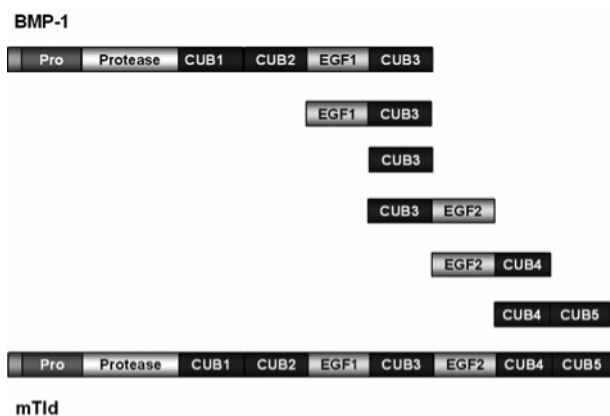


FIGURE 1: Design of constructs for expression in *E. coli* BL21-(DE3) cells. Domain structure of BMP-1 (bone morphogenetic protein) and mTld (mammalian tollid). Pro is the propeptide, protease the astacin-like zinc proteinase domain, CUB the β -sandwich domain named after its occurrence in complement proteins (C1s and C1r), sea urchin UEGF protein, and BMP-1, and EGF the epidermal growth factor-like domain. The longer splice form, mTld, contains additionally the EGF2, CUB4, and CUB5 domains. Depicted between the two splice forms are the constructs chosen for expression in *E. coli*.

min. Equivalent volumes of analyte at the same flow rate were injected over a blank surface treated with the coupling chemistry as a control, which was subtracted as the bulk refractive index background. Regeneration of surfaces was achieved with several 1 min pulses of 0.01 M NaOH. The chosen regeneration conditions were not hazardous to the immobilized material as indicated by reproducible binding results for repeated measurements of a given concentration. Sensorgrams were analyzed using BIAevaluation version 3.1 (BiaCore, Freiburg, Germany). A 1:1 binding model was used for kinetic analysis of all interactions. The apparent equilibrium dissociation constants (K_D) were calculated from the ratio of the dissociation and association rate constants (k_{off}/k_{on}).

RESULTS

Recombinant PCP Domains Can Be Expressed in Bacteria and Purified at High Yields from Bacterial Inclusion Bodies. To clarify the distinct properties of C-terminal PCP domains, we cloned a series of single domains or pairs of domains that successively overlap each other. To obtain answers to the question of why BMP-1 and mTld differ in function, we focused on those subdomains flanking the junction between the short splice variant and the long splice variant (Figure 1). Cultures of pET3a-PCP-transformed *E. coli* BL21(DE3) cells were grown to an E_{600} of 0.7–0.9, induced with IPTG, and harvested after 4 h. Over the observed time period, the amount of expressed protein increased significantly within the molecular size range, whereas expression of the blank pET3a vector did not produce any corresponding protein (Figure 2). The inclusion bodies formed due to the high level of expression were dissolved under reducing conditions in 6 M guanidinium chloride or 8 M urea. The His-tagged proteins were purified by Ni-NTA affinity chromatography in a single peak at pH 4.5 (data not shown). For example, the size of the purified CUB3-EGF2 construct was 20.8 kDa, as determined by SDS gel electrophoresis and Coomassie staining (Figure 3). Hence, the apparent molecular mass for

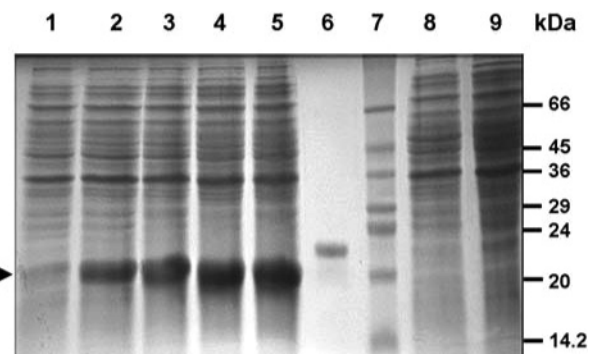


FIGURE 2: Expression of recombinant CUB3-EGF2 in *E. coli* BL21-(DE3). *E. coli* BL21(DE3) cells were transformed with recombinant pET3a, containing PCP constructs, or with pET3a plasmids alone. Samples of expression were submitted to SDS-PAGE analysis (15% SDS-PAGE) and Coomassie stained. In lanes 1–5, samples of expression with recombinant pET3a were collected 0, 1, 2, 3, and 4 h after IPTG induction, respectively. Lane 6 contained the crayfish astacin standard (22.6 kDa, 2.5 μ g). Lane 7 contained the protein standard (Sigma). In lanes 8 and 9, samples of expression with pET3a plasmids alone were collected 0 and 4 h after induction by IPTG, respectively (negative control). Obviously, the amount of recombinant CUB3-EGF2 increases with time (arrow), while there is no increase in the amount of detectable protein in the corresponding range of the negative control.

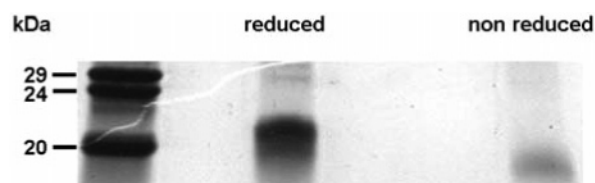


FIGURE 3: SDS-PAGE analysis of recombinant CUB/EGF PCP modules. Folded CUB3-EGF2 was run through a 15% SDS-PAGE gel under reducing and nonreducing conditions: lane 1, reduced protein standard (Sigma); lane 2, reduced CUB3-EGF2; and lane 3, unreduced CUB3-EGF2. A slight shift from a higher molecular mass in the presence of DTT to an apparently lower molecular mass in its absence indicates a more compact folding of the nonreduced proteins and reveals that intrachain disulfide bonds have been formed within the domains rather than interchain ones between them.

recombinant CUB3-EGF2 is within experimental error of its theoretical molecular mass (18.1 kDa). The purified recombinant proteins were submitted to Edman degradation, resulting in a sequence identical to the known N-terminal sequence of each domain (sequence reference, SwissProt accession number P13497). In addition, CUB3-EGF2, EGF2-CUB4, and CUB4-CUB5 fragments were identified by mass spectrometry (data not shown).

The Domains Can Be Folded into Their Native, Functional Conformation. For folding, the recombinant proteins were dialyzed against a buffer devoid of urea, guanidinium chloride, DTT, or β -mercaptoethanol. The folding state of the recombinant proteins was checked by fluorescence and circular dichroism spectroscopy. The tryptophan fluorescence of each domain undergoes a typical red shift due to the change from a nonpolar to a polar environment upon the transition from the folded to the unfolded state. CUB3-EGF2, for instance, shows a shift from 348 to 355 nm (Figure 4). Simultaneously, a significant increase in fluorescence was observed as would be expected for the dequenching effect of unfolding (Figure 4). CD spectra obtained between 205 and 260 nm indicated a mainly antiparallel β -sheet structure

Table 1: Secondary Structure Composition of Folded PCP Domains

secondary structure element ^a	EGF1-CUB3	CUB3	CUB3-EGF2	EGF2-CUB4	CUB4-CUB5
aperiodic	35.3%	34.9%	35.0%	36.0%	34.2%
α -helical	7.3%	5.4%	5.5%	7.3%	5.9%
β -antiparallel	31.2%	42.6%	36.7%	32.2%	34.0%
β -parallel	5.3%	5.5%	5.3%	5.4%	5.2%
β -turn	22.1%	15.8%	20.4%	22.0%	20.8%
sum of β -structures	58.6%	63.9%	62.4%	59.6%	60.0%

^a Obtained from CD spectroscopy (from 205 to 260 nm). See Figure 4.

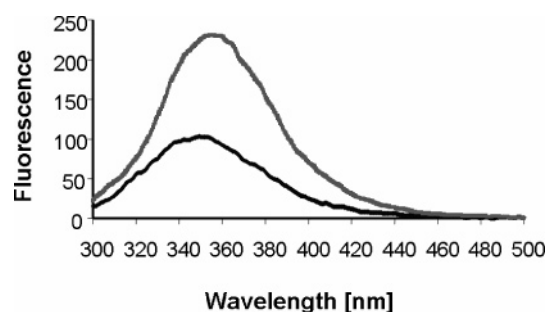


FIGURE 4: Fluorescence emission spectra of folded and unfolded CUB3-EGF2. Fluorescence spectra of folded and unfolded CUB3-EGF2 were recorded in 5 mM ammonium acetate (pH 8.2) (black) or 8 M urea, 150 mM NaCl, and 50 mM Tris-HCl (pH 4.5) (gray). Upon excitation at 280 nm (5 °C), emission was monitored from 300 to 500 nm. Values of 10 scans were averaged. As exemplified for CUB3-EGF2, a red shift from 348 to 355 nm and a significant dequenching effect were observed, depicting the transition from the folded to the unfolded (denatured) state. This is indicative of a nativelike structure of the folded domains.

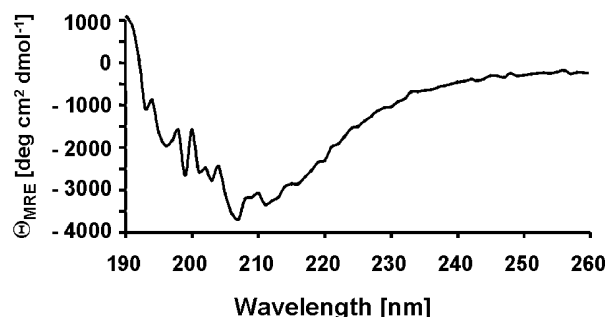


FIGURE 5: Circular dichroism (CD) spectroscopy of PCP domains. Spectra were recorded from 205 to 260 nm at 20 °C at a Jobin-Yvon spectropolarimeter equipped with a cuvette with a path length of 0.5 mm. The protein concentration of CUB3-EGF2 was 0.65 mg/mL. The spectra were corrected by subtracting the buffer spectra. The data were used for deconvolution using CDNN (38) to determine secondary structure elements (see Table 1).

for all domains (shown for CUB3-EGF2 in Figure 5). The estimated β -content ranged between 59 and 64% (Table 1). Further investigations of refolded recombinant proteins on a 15% SDS gel revealed a shift from a higher molecular mass in the presence of the reducing agent dithiothreitol (DTT) to an apparently lower molecular mass in its absence (Figure 3). This behavior provides evidence for the presence of intrachain disulfide bridges within the individual domains rather than interchain ones between them.

The Affinity of C-Terminal CUB/EGF PCP Constructs for Procollagen I Is Stronger than That for Collagen I, the EGF Domains Enhance Affinity, and EGF2-CUB4 (Present in mTld Only, but Not in BMP-1) Binds Most Tightly. The

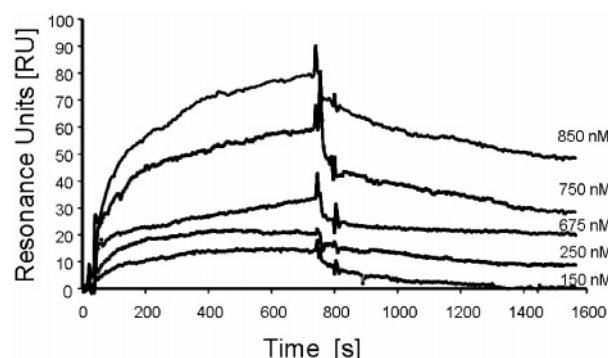


FIGURE 6: Binding of recombinant human EGF1-CUB3 to human procollagen I. Representative sensorgram (after background subtraction) illustrating the interaction of EGF1-CUB3 with procollagen I. EGF1-CUB3 [at 150, 250, 675, 750, and 850 nM, dissolved in 0.01 M Hepes (pH 7.4), 0.15 M NaCl, 5 mM CaCl₂, and 0.005% polysorbate 20 (v/v)] was passed over immobilized procollagen I (780 RU) for 12 min at a flow rate of 5 μ L/min followed by buffer alone. After background subtraction, a 1:1 binding model with a drifting baseline was calculated using BIAevaluation version 3.1 for the kinetic analysis of all interactions. The apparent equilibrium dissociation constants (K_D) were calculated from the ratio of the dissociation and association rate constants (see Table 2).

Table 2: Kinetic Constants for the Interaction of C-Terminal PCP Domains with Procollagen I and Collagen I

substrate	PCP module	k_{on} (M ⁻¹ s ⁻¹)	k_{off} (s ⁻¹)	K_D^a (nM)	χ^2
procollagen I	EGF1-CUB3	4.3×10^4	3.4×10^{-3}	77.8	1.8
	CUB3	3.5×10^3	2.2×10^{-3}	622.0	0.2
	CUB3-EGF2	7.3×10^4	6.7×10^{-4}	9.2	0.4
	EGF2-CUB4	6.7×10^3	6.6×10^{-6}	1.0	1.3
	CUB4-CUB5	3.7×10^3	1.6×10^{-3}	442.0	0.9
collagen I	EGF1-CUB3	8.3×10^3	1.2×10^{-3}	141.0	0.6
	CUB3	2.3×10^3	1.1×10^{-3}	461.0	0.2
	CUB3-EGF2	3.9×10^4	2.6×10^{-3}	68.3	2.0
	EGF2-CUB4	205.0	5.3×10^{-5}	259.0	0.5
	CUB4-CUB5	14.6	9.9×10^{-6}	682.0	0.7

^a Dissociation constants were determined from ratio of kinetic rate constants (k_{off}/k_{on}).

ability of the recombinant PCP domains to bind procollagen I and collagen I was analyzed by a surface plasmon resonance methodology. As exemplified by the interaction of EGF1-CUB3 with procollagen I (Figure 6), the PCP domains bind to immobilized procollagen I and collagen I in a concentration-dependent manner. The association and dissociation rate constants were recorded at protein–ligand concentrations ranging between 0.15 and 1.3 μ M (Table 2). The association and dissociation phases were satisfactorily fitted ($\chi^2 = 0.2–2.0$) simultaneously for all curves using a 1:1 binding model. The addition of mass transport did not improve the fit. A first observation was that CUB -domains devoid of flanking

EGF domains interact only weakly with both procollagen I and collagen I. The corresponding dissociation constants of CUB3 and CUB4-CUB5 are 622 and 442 nM for procollagen I and 461 and 682 nM for collagen I, respectively. In contrast, the binding to procollagen I of such modules that contain EGF1 or EGF2 domains is much tighter. However, these domains exhibit only weak affinity for the product of cleavage, collagen I. This difference is most striking for EGF2-CUB4, which binds procollagen I ~250 times tighter than collagen I ($K_D = 259$ and 1 nM, respectively). Interestingly, among the EGF-containing modules, the binding affinities decrease with an increase in the distance from the C-terminus (Figure 1). The dissociation constant for EGF2-CUB4 ($K_D = 1$ nM) is ~1 order of magnitude tighter than for CUB3-EGF2 ($K_D = 9.2$ nM), and the latter binds another order of magnitude more tightly than EGF1-CUB3 ($K_D = 77.8$ nM). A comparison of the corresponding k_{on} and k_{off} values reveals that a very slow k_{off} value ($6.6 \times 10^{-6} \text{ s}^{-1}$) of EGF2-CUB4 might be responsible for this behavior (Table 2).

DISCUSSION

The C-terminal CUB domains and EGF-like domains of the PCP have been proposed previously to contain exosites for substrate recognition on the basis of the interaction of proteolytic PCP fragments with procollagen I (34). In this study, we have investigated the role of five individual CUB/EGF modules and CUB domains in the interaction of the C-proteinase with its substrate procollagen I in comparison to the product collagen I. The five constructs overlap each other and span the junction between the short splice variant BMP1 and the long splice variant mTld. Hence, they are suitable tools for addressing the question of why BMP-1 is a more efficient C-proteinase than mTld.

The individual constructs were overexpressed in *E. coli*, purified from inclusion bodies, and folded into their functional conformation for surface plasmon resonance binding studies on immobilized procollagen I and mature collagen I. The bacterial system was chosen because experiences in our laboratory and other laboratories (35) had shown that shorter fragments of the C-proteinase were not secreted properly in eukaryotic expression systems. Fluorescence spectra of the recombinant CUB/EGF domains indicated that the domains could be successfully folded into individual entities with higher electrophoretic mobility in the unreduced than in the reduced state, indicating the formation of intramolecular disulfide bridges. These data are in accordance with observations on intact PCP-2/mTld and proteolytic fragments thereof (34), and on the CUB1-EGF module of C1s (31). Moreover, circular dichroism spectra revealed a mainly antiparallel β -sheet structure for the folded modules, which is consistent with structural data (31, 34, 41).

We provide evidence that recombinant EGF1-CUB3, CUB3, CUB3-EGF2, EGF2-CUB4, and CUB4-CUB5 interact with immobilized procollagen I and collagen I in a concentration-dependent manner. The data can be fit implicating a 1:1 stoichiometry, which has also been observed for the binding of the procollagen C-proteinase enhancer protein (PCPE) to procollagen I and to the C-propeptide of procollagen III (42). Likewise, our binding data are in accordance with the binding of intact procollagen I to the

immobilized C-proteinase enhancer [$k_{on} = 5.5 \times 10^4 \text{ M}^{-1} \text{ s}^{-1}$, $k_{off} = 6.2 \times 10^{-5} \text{ s}^{-1}$, and $K_D = 1.1 \text{ nM}$ (42)]. There are slight differences in the corresponding dissociation kinetics, while the k_{on} values are quite similar. Taken together, the C-proteinase enhancer ($K_D = 1.13 \text{ nM}$) exhibits a higher binding affinity for procollagen I than EGF1-CUB3 ($K_D = 77.8 \text{ nM}$) and CUB3-EGF2 ($K_D = 9.21 \text{ nM}$) but binds with an affinity similar to that of EGF2-CUB4 ($K_D = 1.0 \text{ nM}$).

The binding data show that the two EGF-like domains are essential for binding. EGF1-CUB3, CUB3-EGF2, and EGF2-CUB4 bind procollagen I with dissociation constants of 77.8, 9.2, and 1.0 nM, respectively. By contrast, with K_D values ranging between 442.0 and 682.0 nM, the CUB3 domain and the CUB4-CUB5 module devoid of flanking EGF1 or EGF2 are interacting much more weakly with both collagen I and procollagen I. The weak affinity of recombinant CUB4-CUB5 confirms earlier observations, showing that a proteolytic mTld fragment comprising CUB1–CUB5 bound to immobilized procollagen I, whereas a fragment consisting merely of the CUB4 and CUB5 domains did not (34). In light of these binding constants, a combination of a CUB domain and an EGF-like domain appears to serve as the minimal functional unit for protein–protein interactions of the C-proteinase. A similar scenario has been reported for the complement protein C1r whose CUB1-EGF fragment is the minimal segment required for Ca^{2+} -dependent interaction with C1s (43). Most probably, the EGF domains of the C-proteinase and C1s have a similar antiparallel β -sheet fold, since they show a high degree of overall sequence identity, including the Ca^{2+} -binding consensus region (4, 6, 9, 29–32). However, EGF deletion mutants of the C-proteinase retained their Ca^{2+} dependence (37), indicating the presence of additional Ca^{2+} binding sites in the CUB domains and/or the catalytic domain.

Although those domains containing EGF1 or EGF2 bind more tightly to procollagen I than to collagen I, they also bind, albeit more weakly, to collagen I (Table 2). Therefore, binding seems to occur not only to the C-propeptide of procollagen I but also to areas proximal to the C-propeptide cleavage site, possibly in the telopeptide region. A similar behavior has also been reported for the interaction of the C-proteinase enhancer protein with the C-propeptides of procollagen I and procollagen III, and with partially processed pN-collagen I (42).

Another important observation was that the binding affinity of the EGF-containing modules increases with an increase in the distance to the N-terminus (Figure 1). The tightest association is seen in the interaction of procollagen with EGF2-CUB4 ($K_D = 1$ nM), a fragment which is only present in the long splice form mTld. In essence, this would imply that the long splice form mTld binds more tightly to procollagen I than the short splice form BMP-1 does. This is corroborated by the observation that mTld indeed binds more strongly to the extracellular matrix (in general) than does BMP-1 (44).

Nevertheless, it appears paradoxical that BMP-1 is a more efficient C-proteinase than mTld and that the latter is not able to cleave certain substrates (like chordin), which are substrates of BMP-1 (20, 37). In this context, it is remarkable that a truncated C-proteinase, which was terminated after the CUB2 domain, still retained ~80% activity (compared

to BMP-1), which means that the domains beyond CUB2 are not needed for the processing of many C-proteinase substrates (35). In a recent paper (37), Kadler and co-workers suggested that one reason for this paradoxical behavior might be a special hairpin conformation of the long splice form that bends back the CUB4-CUB5 moiety into the vicinity of the catalytic domain and thereby might sterically prevent access of the protease to certain substrates. The hairpin was suggested to be triggered by the EGF-like domains, especially EGF2, which should confer rigidity to the overall conformation of mTld (37). This is an intriguing hypothesis, which would nicely explain several of the functional differences of BMP-1 and mTld. On the other hand, some questions remain unsolved. For example, there are homologues of mTld in *Drosophila* (fly) (22), *Xenopus* (frog) (18, 19), and *Danio* (fish) (21) and even in mammals (mammalian tolloid like-1, mTll-1), which process homologues of mammalian chordin. The fly, frog, and fish enzymes as well as mTll-1 have a domain composition identical to that of human mTld and nevertheless cleave the corresponding growth factor antagonists, which mTld and likewise mTll-2 do not cleave (45). Domain swapping experiments have shown that the protease domain of mTll-2 can cleave chordin if coupled to the CUB1 domain of BMP-1 (45). Likewise, swaps of the catalytic domains between *Drosophila* tolloid (Tld) and tolloid related (Trl) did not change substrate specificity essentially (46), which again supports the view that the C-terminal domains are crucial for substrate recognition.

Hence, we complement these hypotheses with a model which takes into account the different binding affinities of the C-terminal modules of mTld and BMP-1. We hypothesize that due to the presence of the additional EGF2 domain and the CUB4 domain the long splice form mTld binds more tightly to procollagen I. It appears most likely that the interaction involves the C-propeptides, because the binding of the EGF2-CUB4 module to procollagen I is ~250 times stronger than that to collagen I. This might result in a certain degree of product inhibition (by the propeptides), virtually reducing the enzymatic activity as compared to that of BMP-1. This model would complement the observations of Hulmes and co-workers (42), who found that the procollagen C-proteinase enhancer binds to the C-propeptides of procollagen III. It has been reported that procollagen processing already starts within the cell in the late trans-Golgi compartment after the activation of the procollagen C-proteinase by a furin-like prohormone convertase (47, 48). In this scenario, a role for the enhancer could be the interruption of the tight interaction of mTld with procollagen and thereby an up-regulation of mTld activity. This idea is supported by a recent paper in which Greenspan's group demonstrated the binding of the C-proteinase enhancer protein 1 (PCPE-1) to the full-length form of mammalian tolloid-like 1 (mTll-1), which has the same domain composition as mammalian tolloid. By contrast, a shorter version of mTll-1, truncated after the CUB3 domain, failed to bind and was not enhanced by PCPE-1 (36). The importance of the C-terminal EGF2-CUB4-CUB5 region for the recognition and processing of its substrate short gastrulation (SOG) has also been shown for *Drosophila* tolloid (49).

REFERENCES

- Hojima, Y., van der Rest, M., and Prockop, D. J. (1985) Type I procollagen carboxyl-terminal proteinase from chick embryo tendons. Purification and characterization, *J. Biol. Chem.* 260, 15996–6003.
- Kessler, E., and Adar, R. (1989) Type I procollagen C-proteinase from mouse fibroblasts. Purification and demonstration of a 55-kDa enhancer glycoprotein, *Eur. J. Biochem.* 186, 115–21.
- Wozney, J. M., Rosen, V., Celeste, A. J., Mitsock, L. M., Whitters, M. J., Kriz, R. W., Hewick, R. M., and Wang, E. A. (1988) Novel regulators of bone formation: Molecular clones and activities, *Science* 242, 1528–34.
- Takahara, K., Lyons, G. E., and Greenspan, D. S. (1994) Bone morphogenetic protein-1 and a mammalian tolloid homologue (mTld) are encoded by alternatively spliced transcripts which are differentially expressed in some tissues, *J. Biol. Chem.* 269, 32572–8.
- Kessler, E., Takahara, K., Biniaminov, L., Brusel, M., and Greenspan, D. S. (1996) Bone morphogenetic protein-1: The type I procollagen C-proteinase, *Science* 271, 360–2.
- Li, S. W., Sieron, A. L., Fertala, A., Hojima, Y., Arnold, W. V., and Prockop, D. J. (1996) The C-proteinase that processes procollagens to fibrillar collagens is identical to the protein previously identified as bone morphogenetic protein-1, *Proc. Natl. Acad. Sci. U.S.A.* 93, 5127–30.
- Janitz, M., Heiser, V., Bottcher, U., Landt, O., and Lauster, R. (1998) Three alternatively spliced variants of the gene coding for the human bone morphogenetic protein-1, *J. Mol. Med.* 76, 141–6.
- Imamura, Y., Steiglit, B. M., and Greenspan, D. S. (1998) Bone morphogenetic protein-1 processes the NH₂-terminal propeptide, and a furin-like proprotein convertase processes the COOH-terminal propeptide of pro- α 1(V) collagen, *J. Biol. Chem.* 273, 27511–7.
- Kessler, E., Fichard, A., Chanut-Delalande, H., Brusel, M., and Ruggiero, F. (2001) Bone morphogenetic protein-1 (BMP-1) mediates C-terminal processing of procollagen V homotrimer, *J. Biol. Chem.* 276, 27051–7.
- Unsöld, C., Pappano, W. N., Imamura, Y., Steiglit, B. M., and Greenspan, D. S. (2002) Biosynthetic processing of the pro- α 1(V)- α 2(V) collagen heterotrimer by bone morphogenetic protein-1 and furin-like proprotein convertases, *J. Biol. Chem.* 277, 5596–602.
- Medeck, R. J., Sosa, S., Morris, N., and Oxford, J. T. (2003) BMP-1-mediated proteolytic processing of alternatively spliced isoforms of collagen type XI, *Biochem. J.* 376, 361–8.
- Scott, I. C., Imamura, Y., Pappano, W. N., Troedel, J. M., Recklies, A. D., Roughley, P. J., and Greenspan, D. S. (2000) Bone morphogenetic protein-1 processes biglycan, *J. Biol. Chem.* 275, 30504–11.
- Rattenholl, A., Pappano, W. N., Koch, M., Keene, D. R., Kadler, K. E., Sasaki, T., Timpl, R., Burgeson, R. E., Greenspan, D. S., and Bruckner-Tuderman, L. (2002) Proteinases of the bone morphogenetic protein-1 family convert procollagen VII to mature anchoring fibril collagen, *J. Biol. Chem.* 277, 26372–8.
- Amano, S., Scott, I. C., Takahara, K., Koch, M., Champiaud, M. F., Gerecke, D. R., Keene, D. R., Hudson, D. L., Nishiyama, T., Lee, S., Greenspan, D. S., and Burgeson, R. E. (2000) Bone morphogenetic protein 1 is an extracellular processing enzyme of the laminin 5 γ 2 chain, *J. Biol. Chem.* 275, 22728–35.
- Veitch, D. P., Nokelainen, P., McGowan, K. A., Nguyen, T. T., Nguyen, N. E., Stephenson, R., Pappano, W. N., Keene, D. R., Spong, S. M., Greenspan, D. S., Findell, P. R., and Marinkovich, M. P. (2003) Mammalian tolloid metalloproteinase, and not matrix metalloproteinase 2 or membrane type 1 metalloproteinase, processes laminin-5 in keratinocytes and skin, *J. Biol. Chem.* 278, 15661–8.
- Panchenko, M. V., Stetler-Stevenson, W. G., Trubetskoy, O. V., Gacheru, S. N., and Kagan, H. M. (1996) Metalloproteinase activity secreted by fibrogenic cells in the processing of prolysin oxidase. Potential role of procollagen C-proteinase, *J. Biol. Chem.* 271, 7113–9.
- Uzel, M. I., Shih, S. D., Gross, H., Kessler, E., Gerstenfeld, L. C., and Trackman, P. C. (2000) Molecular events that contribute to lysyl oxidase enzyme activity and insoluble collagen accumulation in osteosarcoma cell clones, *J. Bone Miner. Res.* 15, 1189–97.

18. Piccolo, S., Agius, E., Lu, B., Goodman, S., Dale, L., and De Robertis, E. M. (1997) Cleavage of Chordin by Xolloid metalloprotease suggests a role for proteolytic processing in the regulation of Spemann organizer activity, *Cell* 91, 407–16.
19. Goodman, S. A., Albano, R., Wardle, F. C., Matthews, G., Tannahill, D., and Dale, L. (1998) BMP1-related metalloproteinases promote the development of ventral mesoderm in early *Xenopus* embryos, *Dev. Biol.* 195, 144–57.
20. Scott, I. C., Blitz, I. L., Pappano, W. N., Imamura, Y., Clark, T. G., Steiglit, B. M., Thomas, C. L., Maas, S. A., Takahara, K., Cho, K. W., and Greenspan, D. S. (1999) Mammalian BMP-1/Tolloid-related metalloproteinases, including novel family member mammalian Tolloid-like 2, have differential enzymatic activities and distributions of expression relevant to patterning and skeletogenesis, *Dev. Biol.* 213, 283–300.
21. Blader, P., Rastegar, S., Fischer, N., and Strahle, U. (1997) Cleavage of the BMP-4 antagonist chordin by zebrafish tolloid, *Science* 278, 1937–40.
22. Marques, G., Musacchio, M., Shimell, M. J., Wunnenberg-Stapleton, K., Cho, K. W., and O'Connor, M. B. (1997) Production of a DPP activity gradient in the early *Drosophila* embryo through the opposing actions of the SOG and TLD proteins, *Cell* 91, 417–26.
23. Greenspan, D. S. (2005) Biosynthetic processing of collagen molecules, *Top. Curr. Chem.* 247, 149–83.
24. Suzuki, N., Labosky, P. A., Furuta, Y., Hargett, L., Dunn, R., Fogo, A. B., Takahara, K., Peters, D. M., Greenspan, D. S., and Hogan, B. L. (1996) Failure of ventral body wall closure in mouse embryos lacking a procollagen C-proteinase encoded by *Bmp1*, a mammalian gene related to *Drosophila* tolloid, *Development* 122, 3587–95.
25. Bond, J. S., and Beynon, R. J. (1995) The astacin family of metalloendopeptidases, *Protein Sci.* 4, 1247–61.
26. Stöcker, W., Grams, F., Baumann, U., Reinemer, P., Gomis-Rüth, F.-X., McKay, D. B., and Bode, W. (1995) The metzincins: Topological and sequential relations between the astacins, adamalysins, serralsins, and matrixins (collagenases) define a superfamily of zinc-peptidases, *Protein Sci.* 4, 823–40.
27. Gomis-Rüth, F. X. (2003) Structural aspects of the metzincin clan of metalloendopeptidases, *Mol. Biotechnol.* 24, 157–202.
28. Bork, P., and Beckmann, G. (1993) The CUB domain. A widespread module in developmentally regulated proteins, *J. Mol. Biol.* 231, 539–45.
29. Campbell, B. G., Wootton, J. A., MacLeod, J. N., and Minor, R. R. (1998) Sequence of canine COL1A2 cDNA: Nucleotide substitutions affecting the cyanogen bromide peptide map of the $\alpha 2(I)$ chain, *Arch. Biochem. Biophys.* 357, 67–75.
30. Thielens, N. M., Bersch, B., Hernandez, J. F., and Arlaud, G. J. (1999) Structure and functions of the interaction domains of C1r and C1s: keystones of the architecture of the C1 complex, *Immunopharmacology* 42, 3–13.
31. Gregory, L. A., Thielens, N. M., Arlaud, G. J., Fontecilla-Camps, J. C., and Gaboriaud, C. (2003) X-ray structure of the Ca^{2+} -binding interaction domain of C1s. Insights into the assembly of the C1 complex of complement, *J. Biol. Chem.* 278, 32157–64.
32. Feinberg, H., Uitdehaag, J. C., Davies, J. M., Wallis, R., Drickamer, K., Weis, W. I., Ng, K. K., Kolatkar, A. R., Park-Snyder, S., Clark, D. A., Mitchell, D. A., Torgersen, D., Heise, C. T., Taylor, M. E., Prodolliet, J., Bugner, E., and Feinberg, M. (2003) Crystal structure of the CUB1-EGF-CUB2 region of mannose-binding protein associated serine protease-2, *EMBO J.* 22, 2348–59.
33. Romero, A., Romao, M. J., Varela, P. F., Kolln, I., Dias, J. M., Carvalho, A. L., Sanz, L., Topfer-Petersen, E., and Calvete, J. J. (1997) The crystal structures of two spermadhesins reveal the CUB domain fold, *Nat. Struct. Biol.* 4, 783–8.
34. Sieron, A. L., Tretiakova, A., Jameson, B. A., Segall, M. L., Lund-Katz, S., Khan, M. T., Li, S. W., and Stöcker, W. (2000) Structure and function of procollagen C-proteinase (mTolloid) domains determined by protease digestion, circular dichroism, binding to procollagen type I, and computer modeling, *Biochemistry* 39, 3231–9.
35. Hartigan, N., Garrigue-Antar, L., and Kadler, K. E. (2003) Bone morphogenetic protein-1 (BMP-1). Identification of the minimal domain structure for procollagen C-proteinase activity, *J. Biol. Chem.* 278, 18045–9.
36. Ge, G., Zhang, Y., Steiglit, B. M., and Greenspan, D. S. (2006) Mammalian tolloid-like 1 binds procollagen C-proteinase enhancer protein 1, and differs from bone morphogenetic protein 1 in the functional roles of homologous protein domains, *J. Biol. Chem.* 281, 10786–98.
37. Garrigue-Antar, L., Francois, V., and Kadler, K. E. (2004) Deletion of epidermal growth factor-like domains converts mammalian tolloid into a chordinase and effective procollagen C-proteinase, *J. Biol. Chem.* 279, 49835–41.
38. Yiallourous, I., Grosse Berkhoff, E., and Stöcker, W. (2000) The roles of Glu93 and Tyr149 in astacin-like zinc peptidases, *FEBS Lett.* 484, 224–8.
39. Laemmli, U. K. (1970) Cleavage of structural proteins during the assembly of the head of bacteriophage T4, *Nature* 227, 680–5.
40. Böhm, G., Muhr, R., and Jaenicke, R. (1992) Quantitative analysis of protein far UV circular dichroism spectra by neural networks, *Protein Eng.* 5, 191–5.
41. Varela, P. F., Romero, A., Sanz, L., Romao, M. J., Topfer-Petersen, E., and Calvete, J. J. (1997) The 2.4 Å resolution crystal structure of boar seminal plasma PSP-I/PSP-II: A zona pellucida-binding glycoprotein heterodimer of the spermadhesin family built by a CUB domain architecture, *J. Mol. Biol.* 274, 635–49.
42. Ricard-Blum, S., Bernocco, S., Font, B., Moali, C., Eichenberger, D., Farjanel, J., Burchardt, E. R., van der Rest, M., Kessler, E., and Hulmes, D. J. (2002) Interaction properties of the procollagen C-proteinase enhancer protein shed light on the mechanism of stimulation of BMP-1, *J. Biol. Chem.* 277, 33864–9.
43. Thielens, N. M., Enrie, K., Lacroix, M., Jaquinod, M., Hernandez, J. F., Esser, A. F., and Arlaud, G. J. (1999) The N-terminal CUB-epidermal growth factor module pair of human complement protease C1r binds Ca^{2+} with high affinity and mediates Ca^{2+} -dependent interaction with C1s, *J. Biol. Chem.* 274, 9149–59.
44. Reynolds, S. D., Zhang, D., Puzas, J. E., O'Keefe, R. J., Rosier, R. N., and Reynolds, P. R. (2000) Cloning of the chick BMP1/Tolloid cDNA and expression in skeletal tissues, *Gene* 248, 233–43.
45. Petropoulou, V., Garrigue-Antar, L., and Kadler, K. E. (2005) Identification of the Minimal Domain Structure of Bone Morphogenetic Protein-1 (BMP-1) for Chordinase Activity: CHORDINASE ACTIVITY IS NOT ENHANCED BY PROCOLLAGEN C-PROTEINASE ENHANCER-1 (PCPE-1), *J. Biol. Chem.* 280, 22616–23.
46. Serpe, M., Ralston, A., Blair, S. S., and O'Connor, M. B. (2005) Matching catalytic activity to developmental function: Tolloid-related processes Sog in order to help specify the posterior crossvein in the *Drosophila* wing, *Development* 132, 2645–56.
47. Canty, E. G., Lu, Y., Meadows, R. S., Shaw, M. K., Holmes, D. F., and Kadler, K. E. (2004) Coalignment of plasma membrane channels and protrusions (fibripositors) specifies the parallelism of tendon, *J. Cell Biol.* 165, 553–63.
48. Leighton, M., and Kadler, K. E. (2003) Paired Basic/Furin-like Proprotein Convertase Cleavage of Pro-BMP-1 in the trans-Golgi Network, *J. Biol. Chem.* 278, 18478–84.
49. Canty, E. G., Garrigue-Antar, L., and Kadler, K. E. (2006) A complete domain structure of *Drosophila* tolloid is required for cleavage of short gastrulation, *J. Biol. Chem.* (in press).

BI060228K